

**Toward Continuously Variable Fidelity
Wavelet-based Space/Time Adaptive
DNS/CVS/LES Methodology**

by

A Nejadmalayeri

B.S., Amirkabir University of Technology (Tehran
Polytechnic), 1999

M.S., Wichita State University, 2007

A thesis submitted to the
Faculty of the Graduate School of the
University of Colorado in partial fulfillment
of the requirements for the degree of
Doctor of Philosophy
Department of Mechanical Engineering
2014

This thesis entitled:
Toward Continuously Variable Fidelity Wavelet-based Space/Time Adaptive
DNS/CVS/LES Methodology
written by A Nejadmalayeri
has been approved for the Department of Mechanical Engineering

Oleg V. Vasilyev

Prof. Gregory Beylkin

Prof. Jem N. Corcoran

Prof. Kurt Karl Maute

Prof. Alireza Doostan

Date _____

The final copy of this thesis has been examined by the signatories, and we find that
both the content and the form meet acceptable presentation standards of scholarly
work in the above mentioned discipline.

Nejadmalayeri, A (Ph.D., Mechanical Engineering)

Toward Continuously Variable Fidelity Wavelet-based Space/Time Adaptive DNS/CVS/LES
Methodology

Thesis directed by Prof. Oleg V. Vasilyev

The current work is an attempt to construct a wavelet-based variable fidelity approach that provides a smooth transition amongst Wavelet-based Direct Numerical Simulation (WDNS), Coherent Vortex Simulations (CVS), and Stochastic Coherent Adaptive Large Eddy Simulations (SCALES) based on the notion of spatially and temporally varying wavelet thresholding which is proposed by this work. The methodology provides an automatic transition from WDNS – which provides a direct solution of wavelet filtered Navier-Stokes equations – to coherent/incoherent flow decomposition in the CVS limit to SCALES regime, where the energy containing turbulent motions are resolved while the effect of less energetic motions is modeled. The transition between WDNS, CVS, and SCALES regimes is achieved through two-way feedback between the modeled SGS dissipation (or other dynamically important physical quantity) and the computational mesh. The feedback is based on spatio-temporal variation of the wavelet threshold, where the thresholding level is adjusted on the fly depending on the deviation of local significant SGS dissipation from the user prescribed level. This strategy overcome a major limitation for all wavelet-based multi-resolution schemes: the thresholding criterion is global and does not fully utilize the spatial/temporal intermittency of the turbulent flow. Hence, the aforementioned concept of physics-based spatially variable thresholding in the context of wavelet-based numerical techniques for solving PDEs is introduced. The procedure consists of tracking the wavelet thresholding-factor within a Lagrangian frame by exploiting a Lagrangian Path-Line Diffusive Averaging approach that uses linear averaging along characteristics. This work is a prelim-

inary study towards the construction of continuously variable fidelity wavelet-based space/time/model-form adaptive methodology.

Contents

Chapter

1	Introduction	1
1.1	Motivation	10
1.2	Stochastic Coherent Adaptive Large Eddy Simulation	10
1.2.1	Wavelet Thresholding Filter	11
1.2.2	Wavelet-Filtered Navier-Stokes Equations	12
1.2.3	Localized Kinetic Energy based Model (LKM)	12
2	Spatially Variable Thresholding	15
3	Results	17
4	Perspectives	24
	Bibliography	33

Figures

Figure

1.1 Schematic of Wavelet Threshold Filter	5
1.2 Filtered DNS data on 256^3 grid at $Re_\lambda \approx 168$	6
1.3 Velocity Energy Spectra For Each Wavelet Scale.	7
1.4 Wavelet transform of the Vorticity field. Courtesy of Marie Farge and Kai Schneider [13].	8
1.5 Coherency Diagram: At-a-Glance Comparison of DNS, WDNS, CVS, SCALES, LES.	9
3.1 Time-history of total fraction SGSD.	18
3.2 Time-history of TAF and τ_ϵ^{-1}	19
3.3 Number of Active Wavelets.	21
3.4 Compression Ratio.	21
3.5 Total Resolved Dissipation, $\langle \varepsilon_{\text{res}} \rangle$	21
3.6 Total SGS Dissipation, $\langle \Pi \rangle$	22
3.7 Total Resolved+SGS Dissipation, $\langle \varepsilon_{\text{res}} \rangle + \langle \Pi \rangle$	22
3.8 Taylor Microscale Reynolds Number, Re_λ	22
3.9 Incompressible flow around NACA 0015 at 30° angle-of-attack.	23
4.1 Domain partitioning: (a) geometric simultaneous, (b) geometric sequential, (c) Zoltan geometric, (d) Zoltan hypergraph.	29

4.2	Dynamic Load balancing using Zoltan hypergraph domain partitioning for Convection-Diffusion of Rotating Ellipsoids.	30
4.3	Parallel Speedup for CVS $\epsilon = 0.2$ $\nu = 0.015$ $C_f = 6.6$ $Re_\lambda = 190$ 1024^3 using geometric sequential partitioning.	30

Chapter 1

Introduction

Humorous fable by Horace Lamb, British physicist and applied mathematician, in 1932 just two years before his death in 1934 goes as follows: “I am an old man now, and when I die and go to heaven there are two matters on which I hope for enlightenment. One is quantum electrodynamics, and the other is the turbulent motion of fluids. And about the former I am rather optimistic.”

In the words of the legendary Nobel Prize-winning physicist, Richard Feynman, “Turbulence is the last great unsolved problem of classical physics.”

George Papanicolaou from Stanford University, in an interview with Science Watch correspondent Gary Taubes, to answer the question, “Turbulence theory has not changed much in 30 years. Why is that? Why did Feynman call it the last great unsolved problem?” said: “Simply, turbulence is very hard. Every hard problem in classical physics finds itself embedded in turbulence. It is nonlinear, chaotic, stochastic. And there is no separation of scales – you must deal with a very large number of scales of irregularities. It’s just a mess. In most other physics problems, you can get control by reducing them to simpler problems that you can understand. You can separate scales, for instance, and determine that certain scales are not important. You can limit the phenomena. Or perhaps the inhomogeneity, the chaotic behavior, is not there all the time, so you can somehow approach it. In turbulence all these things happen at once, and you don’t know how to separate them out.”

He still hopes he will be able to “find a way to create numerical computational methods that really use theoretical insight.” He continued “One really interesting problem is to think of clever ways to make numerical calculations that really straddle many scales. So far the numerical calculations have been rather straightforward – direct numerical calculation: write down the equations, put them on the computer, solve them. There have to be more intelligent ways of approaching this, to put more insight into the computer modeling. In the next 10 or 20 years, that’s what’s going to happen. The computational schemes are going to become increasingly intelligent, more adaptive. We are going to put into computer code the ability to recognize its environment and adapt, to become more efficient, and to be guided by the theory. The scant theory that exists right now is not employed in any intrinsic way when you use a computer to help make the problem more efficient. For turbulence it would be enormously important to be able to do that.”

According to Marcel Lesieur [25]: “Turbulence is a dangerous topic which is often at the origin of serious fights in the scientific meetings devoted to it since it represents extremely different points of view, all of which have in common their complexity, as well as an inability to solve the problem. It is even difficult to agree on what exactly is the problem to be solved.”

Lesieur schematically categorized the opposing points of view advocated during last 30 years into 3 communities as follow: 1) **Statistical**: tried to model the evolution of averaged quantities of the flow. This community, which had followed the glorious trail of Taylor and Kolmogorov, believed in the phenomenology of cascades, and strongly disputed the possibility of any coherence or order associated to turbulence; 2) **Coherence among Chaos**: considered turbulence from a purely deterministic point of view, by studying either the behavior of dynamical systems, or the stability of flows in various situations. Experimentalist and computer simulators who sought to identify coherent vortices in flows were also associated to this community; 3) **Emergence of third point**

of view – with the concepts of renormalization group theory, multifractality, mixing, and Lagrangian approaches – pushed by physicists, has made the existence of the first two camps less clear.

This “very hard” (in words of Papanicolaou) and “dangerous” (according to Lesieur) topic by and large has been the center of attention of scientific-computing society and numerical-scheme developers community, although not all the attempts have made precise attention to even a few existing scant theories. The goal of this work is to try to propose improvement techniques in an attempt to construct a numerical scheme which address all aforementioned challenges: mainly to distinguish different scales and to treat them in different consistent fashion while not forgetting even the ignored scales or better to say, being able to include even ignored scales within the same numerical framework in future works.

The numerical techniques for computational simulation of turbulence are mainly categorized as DNS (Direct Numerical Simulation) and LES (Large Eddy Simulation). Direct Numerical Simulation (DNS) is the most accurate numerical approach for solving Navier-Stokes equations using higher-order finite difference/spectral schemes. DNS resolves all the physically meaningful scales within the limit of continuum mechanics from integral length scale all the way down to the smallest dissipative Kolmogorov length scale; however, its formidable computational complexity, $\sim Re^{\frac{9}{4}}$ only for spatial scales, makes it an impossible solution for real flow applications at least by end of this century or perhaps until quantum computers become a reality – “Every time a new supercomputer comes out, people immediately test what it will do for the turbulence problem [1].” It is worth stressing that the largest DNS to date is limited to 4096^3 grid points at $Re \approx 10^6$ performed in 2002 [28].

To tackle the DNS challenges, the notion of Large Eddy Simulation (LES) proposed in which the resolved large scales are simulated deterministically directly (akin to the DNS) while the interaction of large (resolved) with small (unresolved, mod-

eled) scales are modeled like RANS (Raynolds Averaged. Navier-Stokes). The scales distinction is obtained by applying low-pass frequency filters to the Navier-Stokes equations. Throughout the filtering process, filtered Navier-Stokes has more unknowns than number of equations and hence Sub-Grid Scale (SGS) models close the system of the equations via modeling the SGS stresses tensor. Contrary to RANS, only a part of the nonlinear interactions is modeled (by SGS models) in LES. The modeled interactions involve small scales which are generally in the inertial-range and, as a result, have more universal character than flow-dependent large-scales. In spite of its success in enormous degree-of-freedom reduction and distinction of small/large scales, in LES only the large-scales are resolved versus energy-containing-motions which are of more importance. Besides, LES is still expensive if no-slip BCs are used.

Issues like strong temporal/spatial intermittency, localized small structures in spatial/time space, and large range of temporal scales (Integral-scale / Kolmogorov-scale: $\eta = \sqrt[4]{\nu^3/\varepsilon}$) require the need for multi-resolution schemes in turbulence simulations among which wavelet-based techniques are strong candidates due to the prominent wavelet properties including:

Windowed Transform property (temporal/spatial localized change of scale); intrinsic adaptiveness of these schemes simply by switching on/off wavelet coefficients; signal de-noising; existence of fast transform; capability of identification of coherent structures (signature-recognition property); and capturing multiscale (multi-resolution) character of turbulence. That is why the idea of using wavelets in turbulence was proposed for the first time by Marie Farge [12] based on the outstanding wavelets properties.

The way wavelet transform works in general is to decompose a function Fig. 1.1(a) into wavelet-coefficients and wavelet-scaling-functions on different level of resolution at different locations on a dyadic grid Fig. 1.1(b). The way that wavelet-thresholding-filter works is to keep only the grid-points corresponding to the wavelet-coefficients above a priori defined thresholding factor Fig. 1.1(c) and there is no limitation on thresholding-

factor at all, which is an arbitrary non-dimensional positive real-value scalar. The error of this filtering scales as thresholding-factor. To compare the Fourier and wavelet filters from energy-spectra (as in DNS case) standpoint one can see that by cutting at a certain threshold-level, the portion of the spectra which is kept corresponds to a wide range of wavenumbers compared with Fourier-cutoff filter (where we just cut the wavenumbers at a certain frequency), Fig. 1.2. That is because of the fact that each wavelet level (scale) corresponds to a range of wavenumbers, Fig. 1.3.

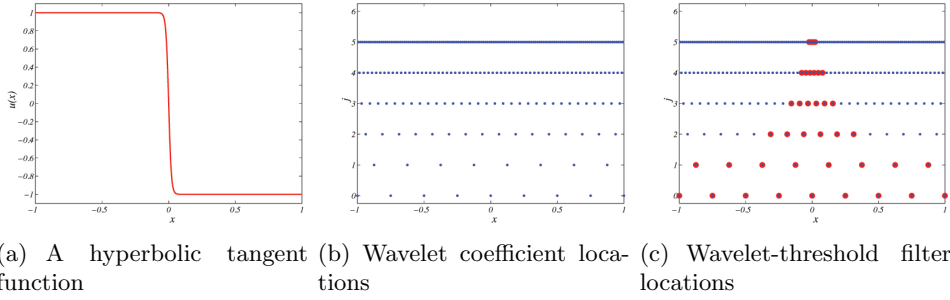


Figure 1.1: Schematic of Wavelet Threshold Filter

The astonishing wavenumber compression due to use of wavelets is evident in a very insightful and artistic illustration, Fig. 1.4, from a work by Farge and Schneider [13] which showed that by transforming the vorticity field into wavelet space, it can be realized that the high-concentration of active-wavelets are appeared only at few spatial locations.

The wavelet based methods mainly categorized into WDNS (Wavelet based DNS), CVS (Coherent Vortex Simulation), and SCALES(Stochastic Coherent Adaptive Large Eddy Simulation).

WDNS – proposed for the first time by Fröhlich and Schneider [23] – is in fact and Adaptive-DNS where the wavelet-based numerical methods used to solve Navier-Stokes equations without any model with a sufficiently small threshold in order to ensure that the ignored-scales are not significant. As a result of wavelet filtering and due

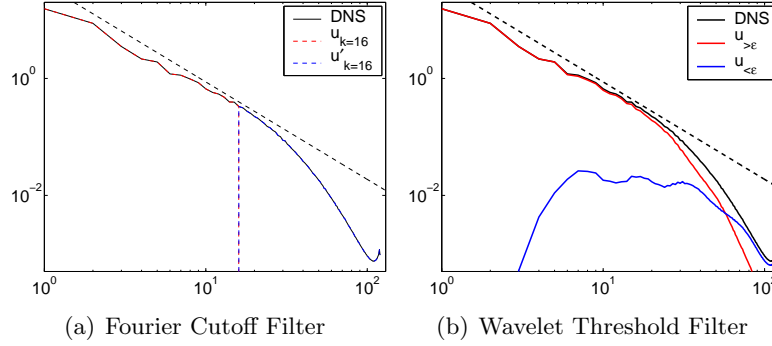


Figure 1.2: Filtered DNS data on 256^3 grid at $Re_\lambda \approx 168$

to compression property of wavelets, the number of DOF (degree-of-freedom) reduced compared with DNS; however, still due to small threshold, it is very expensive or better to say impossible for real flow applications: the 2D spatial computational complexity scales as $Re^{\frac{1}{2}}$.

CVS – proposed by Farge et al. [14] – is based on the idea that coherent modes are the ones which are mostly responsible for the evolution of the turbulence and the fully developed turbulence is made of: 1) an organized coherent part; and 2) a random incoherent part. It was observed that by filtering the vorticity field using orthogonal wavelet bases, the probability density function (PDF) of the unresolved field is of the form of PDF of Gaussian white noise. Therefore, CVS (wavelet-filtered vorticity with an optimal threshold) is an approach to decompose the flow into deterministic and stochastic fields. Therefore, in CVS 1) the coherent-structures (the wavelet de-noised vorticity-field) are simulated directly; and 2) The incoherent-structures is considered as a Gaussian white noise: (“resulting SGS field” by CVS is “near Gaussian white noise”) that provides no turbulent-dissipation.

Stochastic Coherent Adaptive Large Eddy Simulation (SCALES) [16] is a recent wavelet-based methodology for numerical simulations of turbulent flows that resolves energy containing turbulent motions using wavelet multi-resolution decomposition and

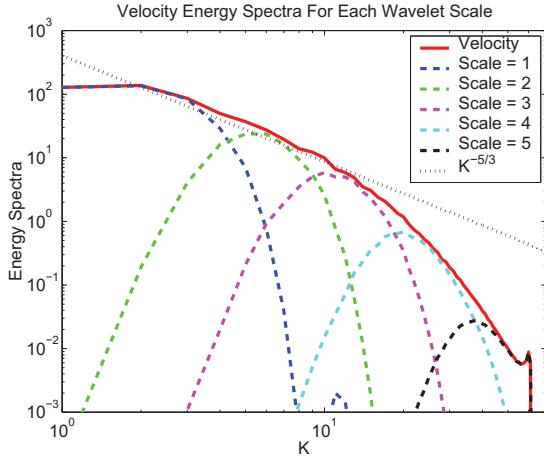


Figure 1.3: Velocity Energy Spectra For Each Wavelet Scale.

self-adaptivity. In this technique, the extraction of the most energetic structures is achieved using wavelet thresholding filter with a priori prescribed threshold level.

SCALES is a methodology, which inherits the advantages of both Coherent Vortex Simulations (CVS) [14] and Large Eddy Simulation (LES) while overcoming the shortcomings of both. Unlike coherent/incoherent and large/small structures decomposition in CVS and LES respectively, in SCALES the separation is between more and less energetic structures. Therefore, unlike CVS, the effect of background flow can not be ignored and needs to be modeled similarly to LES. Furthermore, the filtering and consequently, the subgrid scale (SGS) model are benefited from wavelet nonlinear multiscale band-pass filter, which depends on instantaneous flow realization. As a result of using SGS models, the number of degrees-of-freedom is smaller than CVS and consequently a higher grid-compression can be achieved.

In SCALES, the Navier-Stokes equations are solved using the adaptive wavelet collocation method (AWCM) [35] which is based on the second-generation bi-orthogonal wavelet – a compactly supported and symmetric scheme.

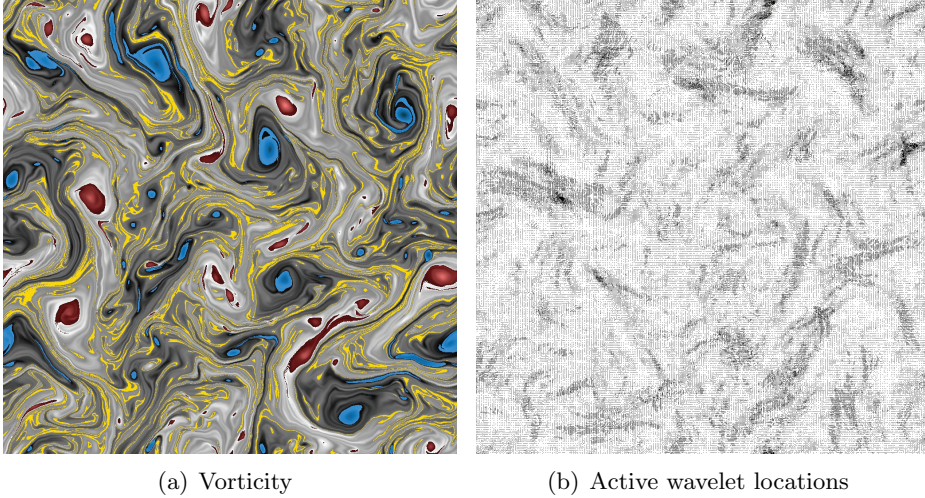


Figure 1.4: Wavelet transform of the Vorticity field. Courtesy of Marie Farge and Kai Schneider [13].

Unlike the CVS which is based on vorticity equations, SCALES similar to LES solves the velocity field and it was proved that using bi-orthogonal wavelets, the PDF of the modeled portion of the SGS (wavelet-filtered out) velocity field is of the form of Gaussian white noise PDF.

This fraction of the less energetic structures is in fact a small part of SGS field. That is to say, the velocity field is initially decomposed to more and less energetic structures by means of wavelet-threshold filter. The “deterministic most energetic coherent structures” are solved directly using AWCM. However, the unresolved field is not absolutely an incoherent stochastic field with no effect on the resolved field and as a result, it needs to be modeled. Again, using wavelet-threshold filter, the unresolved field is decomposed into two kinds of modes: the minority “deterministic coherent SGS modes”; and the “majority stochastic incoherent SGS modes”. The effect of these two modes on the resolved field can be modeled by “deterministic SGS models” and “stochastic SGS models” respectively.

The overall at-a-glance comparison of these wavelet-based methods – WDNS,

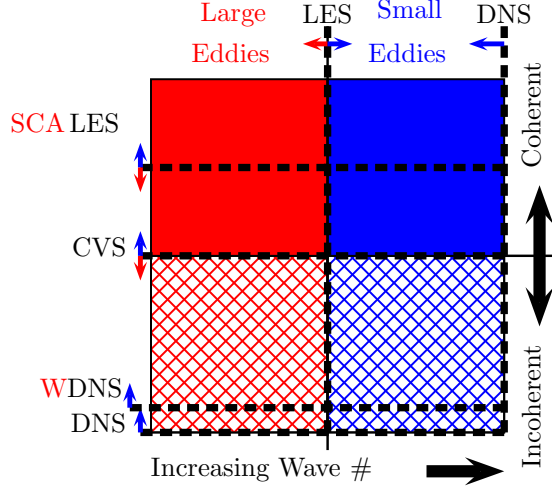


Figure 1.5: Coherency Diagram: At-a-Glance Comparison of DNS, WDNS, CVS, SCALES, LES.

CVS, SCALES – and the non-wavelet-based methods – DNS, LES – can be easily illustrated in Coherency Diagram, Fig. 1.5, on which the wavenumber increase in the horizontal direction and the wavelet-threshold-filter threshold-parameter increase in the vertical direction upward. It is clearly shown that the CVS and LES are limiting case of Coherent/Incoherent and Large/Small structures distinctions while in SCALES in a more relaxed fashion, both resolved and unresolved structures are not limited to these separations. Therefore, while not being limited to homogenous-turbulence – as is the case in CVS – with a very high grid-compression ratio, majority of important energetic structures are resolved and both coherent-deterministic and incoherent-stochastic unresolved modes can be modeled. This distinction is not anymore limited to the size of the structures – which is rather less informative – as it is the case in classical LES. Furthermore, resolved structures and the modeled eddies share a range of wavenumbers together in order to ensure more realistic energy cascades.

1.1 Motivation

Ever since the emergence of the wavelet-based multi-resolution schemes for simulations of turbulence, there has been a major limitation for all wavelet-based techniques: the use of a priori defined global (both in space and time) thresholding-parameter. In this work the robustness of the SCALES approach is further improved by exploring the spatially and temporally variable thresholding strategy, which allows more efficient representation of intermittent flow structures.

1.2 Stochastic Coherent Adaptive Large Eddy Simulation

The properties of wavelet transform, namely the ability to identify and efficiently represent temporal/spatial coherent flow structures, self-adaptiveness, and de-noising, have made them attractive candidates for constructing multi-resolution variable fidelity schemes for simulations of turbulence [34].

To address the shortcomings of LES and CVS, SCALES uses a wavelet thresholding filter to dynamically resolve and track the deterministic most energetic coherent structures while the effect of less energetic unresolved modes is modeled. The unresolved less energetic structures have been shown to be composed of a minority of deterministic coherent modes that dominate the total SGS dissipation and a majority of stochastic incoherent modes that, due to their decorrelation with the resolved modes, add little to the total SGS dissipation [16, 6]. In the current implementation, similar to the classical LES, only the effect of coherent part of the SGS modes is modeled using deterministic SGS models. The use of stochastic SGS models to capture the effect of the incoherent SGS modes will be the subject of future investigations. The most significant feature of SCALES is the coupling of modeled SGS dissipation and the computational mesh: more grid points (active wavelets) are used for SGS models with lower levels of SGS dissipation. In other words, the SCALES approach compensates for inadequate SGS

dissipation by automatically increasing the local resolution and, hence, the level of resolved viscous dissipation. Another noticeable feature of the SCALES method is its ability to match the DNS energy spectra up to the dissipative wavenumber range using considerably less degrees of freedom.

1.2.1 Wavelet Thresholding Filter

In the wavelet-based approach to the numerical simulation of turbulence the separation between resolved energetic structures and unresolved residual flow is obtained through nonlinear multi-resolution wavelet threshold filtering (WTF). The filtering procedure is accomplished by applying the wavelet-transform to the unfiltered velocity field, discarding the wavelet coefficients below a given threshold (ϵ) and transforming back to the physical space. This results in decomposition of the turbulent velocity field into two different parts: a coherent more energetic velocity field and a residual less energetic coherent/incoherent one, i.e., $u_i = \bar{u}_i^{>\epsilon} + u'_i$, where $\bar{u}_i^{>\epsilon}$ stands for the wavelet-filtered velocity at level ϵ

$$\bar{u}_i^{>\epsilon}(\mathbf{x}) = \sum_{l \in \mathcal{L}^0} c_l^0 \phi_l^0(\mathbf{x}) + \sum_{j=0}^{+\infty} \sum_{\mu=1}^{2^n-1} \sum_{\substack{\mathbf{k} \in \mathcal{K}^{\mu,j} \\ |d_{\mathbf{k}}^{\mu,j}| > \epsilon \|u_i\|_{\text{WTF}}}} d_{\mathbf{k}}^{\mu,j} \psi_{\mathbf{k}}^{\mu,j}(\mathbf{x}), \quad (1.1)$$

where $\psi_{\mathbf{k}}^{\mu,j}$ are wavelets of family μ at j level of resolution, $d_{\mathbf{k}}^j$ are the coefficients of the wavelet decomposition, and ϕ_l^0 are scaling functions at zero level of resolution.

The key-role in the wavelet-filter definition is clearly played by the non-dimensional relative thresholding level ϵ that explicitly defines the relative energy level of the eddies that are resolved and, consequently, controls the importance of the influence of the residual field on the dynamics of the resolved motions. In this work we explore the use of spatially and temporary varying thresholding level ϵ , which follows the evolution of the turbulent velocity field.

1.2.2 Wavelet-Filtered Navier-Stokes Equations

By filtering the Navier-Stokes equations, the following SCALES equations that govern the evolution of coherent energetic structures are obtained:

$$\partial_{x_i} \bar{u}_i^{>\epsilon} = 0, \quad (1.2)$$

$$\partial_t \bar{u}_i^{>\epsilon} + \bar{u}_j^{>\epsilon} \partial_{x_j} \bar{u}_i^{>\epsilon} = -\partial_{x_i} \bar{P}^{>\epsilon} + \nu \partial_{x_j x_j}^2 \bar{u}_i^{>\epsilon} - \partial_{x_j} \tau_{ij}^* + Q \bar{u}_i^{>\epsilon}, \quad (1.3)$$

where $\tau_{ij} = \bar{u}_i \bar{u}_j^{>\epsilon} - \bar{u}_i^{>\epsilon} \bar{u}_j^{>\epsilon}$ are the unresolved “SGS stresses” tensor that its Deviatoric part $\tau_{ij}^* = \tau_{ij} - \frac{1}{3} \tau_{kk} \delta_{ij}$ needs to be modeled $Q \bar{u}_i^{>\epsilon}$ is the linear forcing term [27], which is applied in the physical space over the whole range of wavenumbers, and the superscript $(\cdot)^{>\epsilon}$ denotes wavelet filtered quantities. The SCALES equations are similar to the LES ones with the exception that the nonlinear multiscale band-pass wavelet filter, which depends on instantaneous flow realization, is used. The unresolved SGS stresses represent the effect of “unresolved less energetic deterministic coherent and stochastic incoherent eddies” on the “resolved more energetic coherent structures”. In this study the localized kinetic-energy-based model [9] is exploited to close the filtered momentum equations. The SCALES methodology involving both the filtered momentum and the SGS energy equations is implemented by means of the adaptive wavelet collocation method [35].

1.2.3 Localized Kinetic Energy based Model (LKM)

The localized SGS models like LKM, are based on the eddy-viscosity models assumption where turbulent viscosity depends on SGS kinetic energy contrary to the Smagorinsky model in which turbulent viscosity depends on the resolved rate of strain, $\bar{S}_{ij}^{>\epsilon}$. Hence the unknown unresolved “SGS stresses” tensor is approximated as:

$$\tau_{ij}^* \cong -2\nu_t \bar{S}_{ij}^{>\epsilon}. \quad (1.4)$$

In order to define the “turbulent eddy-viscosity” ν_t , one can assume the square root of

SGS kinetic energy as the velocity scale and the wavelet-filter characteristic width Δ as the length scale:

$$\nu_t = C_\nu \Delta k_{\text{sgs}}^{1/2} \quad (1.5)$$

where, C_ν is the Turbulent Eddy-Viscosity Model coefficient. As a result, the deviatoric part of the unresolved “SGS stresses” tensor which needs to be modeled is approximated as:

$$\tau_{ij}^* \cong -2C_\nu \Delta k_{\text{sgs}}^{1/2} \bar{S}_{ij}^{>\epsilon}. \quad (1.6)$$

The SGS-Dissipation – rate of local-transfer of Energy from energetic-resolved-eddies to unresolved-structures – by definition obtained from τ_{ij}^* and $\bar{S}_{ij}^{>\epsilon}$:

$$\Pi = -\tau_{ij}^* \bar{S}_{ij}^{>\epsilon}. \quad (1.7)$$

Hence by replacing approximate (modeled) value for the the Deviatoric part of SGS-stress, SGS-Dissipation rate is approximated in terms of the SGS kinetic energy (SGS K.E.) as:

$$\Pi \cong C_\nu \Delta k_{\text{sgs}}^{1/2} |\bar{S}_{ij}^{>\epsilon}|^2 \quad (1.8)$$

where, resolved rate-of-strain tensor is defined as:

$$\bar{S}_{ij}^{>\epsilon} = \frac{1}{2} \left(\partial_{x_j} \bar{u}_i^{>\epsilon} + \partial_{x_i} \bar{u}_j^{>\epsilon} \right) \quad (1.9)$$

and the modulus of the rate-of-strain tensor is:

$$|\bar{S}^{>\epsilon}|^2 = 2 \bar{S}_{ij}^{>\epsilon} \bar{S}_{ij}^{>\epsilon}. \quad (1.10)$$

The model Transport equation for SGS K.E. is expressed as follows [15]:

$$\frac{\partial k_{\text{sgs}}}{\partial t} + \bar{u}_j^{>\epsilon} \frac{\partial k_{\text{sgs}}}{\partial x_j} = (\nu + \nu_t) \frac{\partial^2 k_{\text{sgs}}}{\partial x_j \partial x_j} - \tilde{\varepsilon}_{\text{sgs}} + \Pi \quad (1.11)$$

where, SGS K.E. is defined as the difference between the wavelet filtered energy $\bar{k}^{>\epsilon}$ and the kinetic energy of the filtered velocity field k_{res} :

$$k_{\text{sgs}} = \bar{k}^{>\epsilon} - k_{\text{res}} = \frac{1}{2} (\bar{u}_i \bar{u}_i^{>\epsilon} - \bar{u}_i^{>\epsilon} \bar{u}_i^{>\epsilon}) \quad (1.12)$$

and SGS viscous dissipation by definition is:

$$\tilde{\varepsilon}_{\text{sgs}} = \nu \left(\frac{\overline{\partial u_i \partial u_i}^{\epsilon}}{\partial x_j \partial x_j} - \frac{\partial \overline{u_i}^{\epsilon}}{\partial x_j} \frac{\partial \overline{u_i}^{\epsilon}}{\partial x_j} \right) = \bar{\varepsilon}^{\epsilon} - \tilde{\varepsilon}_{\text{res}}. \quad (1.13)$$

Where, $\tilde{\varepsilon}_{\text{res}} = \nu \partial_{x_j} \overline{u_i}^{\epsilon} \partial_{x_j} \overline{u_i}^{\epsilon}$ is the resolved pseudo-dissipation and $\varepsilon_{\text{res}} = 2\nu \overline{S_{ij}}^{\epsilon} \overline{S_{ij}}^{\epsilon}$ is resolved turbulent dissipation

Similar to the SGS stress model, the SGS viscous dissipation can be modeled using simple scaling arguments:

$$\tilde{\varepsilon}_{\text{sgs}} = C_{\varepsilon} \Delta^{-1} k_{\text{sgs}}^{3/2}. \quad (1.14)$$

This modeling procedure results in two dimensionless model coefficients (parameters): “Turbulent Eddy-Viscosity Model Coefficient” C_{ν} and “SGS Energy Dissipation Model Coefficient” C_{ε} . Based on previous numerical studies [9], for the sake of simplicity and saving computational resources, in the current effort, the model parameters are assumed to be priori prescribed constants as: $C_{\varepsilon} = 1.0$ and $C_{\nu} = 0.06$.

Chapter 2

Spatially Variable Thresholding

Previous studies, e.g. [17], demonstrated that in SCALES, the SGS dissipation is proportional to ϵ^2 ; therefore, one can enhance SCALES by exploiting spatially-varying ϵ based on local SGS dissipation $\Pi = -\tau_{ij}^* \bar{S}_{ij}^{>\epsilon}$. This implies that rate of local-transfer of energy from energetic-resolved-eddies to unresolved-less-energetic structures can be controlled by varying the thresholding-factor. Therefore, the idea is to locally vary ϵ wherever Π deviates from a priori defined goal-value. A decrease of the thresholding level results in the local grid refinement with subsequent rise of the resolved viscous dissipation, while an increase of ϵ coarsens the mesh resulting in the growth of the local SGS dissipation. However, in order to vary ϵ in a physically consistent fashion, it should follow the local flow structures as they evolve in space and time. This necessitates the Lagrangian representation of ϵ , which is achieved using the Lagrangian Path-Line Diffusive Averaging approach [36]:

$$\partial_t \epsilon + \bar{u}_j^{>\epsilon} \partial_{x_j} \epsilon = -\text{forcing}_{\text{term}} + \nu_\epsilon \partial_{x_j x_j}^2 \epsilon. \quad (2.1)$$

For the sake of efficiency, instead of solving Eq. (2.1) for the evolution of ϵ , the linear-interpolation along characteristics, similar to the idea of Meneveau et. al [30], is performed

$$\frac{1}{\Delta t} \left[\epsilon^{\text{new}}(\mathbf{x}, t + \Delta t) - \epsilon^{\text{old}}(\mathbf{x} - \bar{\mathbf{u}}^{>\epsilon} \Delta t, t) \right] = -\text{forcing}_{\text{term}}. \quad (2.2)$$

The use of linear interpolation results in sufficient numerical diffusion, thus, eliminating the need for explicit diffusion. The proposed spatially variable thresholding strategy ensures that the wavelet threshold is not **a priori** prescribed but determined on the fly by desired turbulence resolution. In this work two different mechanisms for the forcing term are studied:

FT1 The local fraction SGSD (FSGSD) is defined as $\frac{\Pi}{\varepsilon_{\text{res}} + \Pi}$, where $\varepsilon_{\text{res}} = 2\nu \bar{S}_{ij}^{>\epsilon} \bar{S}_{ij}^{>\epsilon}$ is the resolved viscous dissipation. The idea is to maintain FSGD at a “Goal” value which means retain Π at $\varepsilon_{\text{res}} \frac{\text{Goal}}{1-\text{Goal}}$. The first forcing type (FT1) is an attempt to implement this while normalizing the forcing term based on its time average:

$$\text{forcing}_{\text{term}} = \epsilon^{\text{old}} (\mathbf{x} - \bar{\mathbf{u}}^{>\epsilon} \Delta t, t) C_{f_\epsilon} \frac{\Pi - \varepsilon_{\text{res}} \frac{\text{Goal}}{1-\text{Goal}}}{\text{TAF}}, \quad (2.3)$$

where TAF stands for the time average of the forcing, is the time average of $|\Pi - \varepsilon_{\text{res}} \frac{\text{Goal}}{1-\text{Goal}}|$. The forcing constant coefficient, C_{f_ϵ} , is intentionally set to 400 in order to make the time response of FT1 about three to four times faster than large eddy turnover time which is discussed in the next section.

FT2 In this approach, the variations of local-FSGSD is controlled directly based on the goal-value in conjunction with a relaxation time parameter (time-scale), τ_ϵ ,

$$\text{forcing}_{\text{term}} = \epsilon^{\text{old}} (\mathbf{x} - \bar{\mathbf{u}}^{>\epsilon} \Delta t, t) \frac{1}{\tau_\epsilon} \left(\frac{\Pi}{\varepsilon_{\text{res}} + \Pi} - \text{Goal} \right). \quad (2.4)$$

Following the time-varying threshold studies [7], a time-scale associated to the characteristic rate-of-strain is chosen: $\tau_\epsilon^{-1} = \langle |\bar{S}_{ij}^{>\epsilon}| \rangle$.

Chapter 3

Results

The proposed methodology has been tested for linearly forced homogeneous turbulence [8] with linear forcing constant coefficient $Q = 6$ at $Re_\lambda \cong 72$ (Taylor micro-scale Reynolds number) using localized dynamic kinetic-energy-based SGS models [9, 8] on an adaptive grid with effective resolution 256^3 . Figure 3.1 demonstrates the preliminary results of this implementation for three different goal-values (0.4, 0.3, 0.25) for the local FSGSD with the upper and lower bound for epsilon set as 0.2 and 0.43 ($\epsilon \in [0.2, 0.43]$) as well as a constant-thresholding case of $\epsilon = 0.43$. The local and total FSGSD are defined respectively as $\frac{\Pi}{\varepsilon_{\text{res}} + \Pi}$ and $\frac{\langle \Pi \rangle}{\langle \varepsilon_{\text{res}} \rangle + \langle \Pi \rangle}$, where $\langle \Pi \rangle = \langle -\tau_{ij}^* \bar{S}_{ij}^{>\epsilon} \rangle$ and $\langle \varepsilon_{\text{res}} \rangle = 2\nu \langle \bar{S}_{ij}^{>\epsilon} \bar{S}_{ij}^{>\epsilon} \rangle$ are respectively the volume-averaged SGS dissipation and the volume-averaged resolved viscous dissipation .

For the case of Goal=0.4, total-FSGSD never reaches the prescribed goal-value (0.4). The reason is that the total-FSGSD for the case of constant-thresholding with $\epsilon = 0.43$ is than 0.4 for most of the time. As a result, varying thresholding-factor with a “local-FSGSD goal-value” larger than the average FSGSD of constant-thresholding using the same ϵ and ϵ_{max} resulted in total-FSGSD, which was bellow the goal-value. Similarly to the previous case, the test case of the goal-value of 0.3 inherits a large-period oscillations due to capping ϵ at 0.43 level regardless of the forcing method. These oscillations are removed by increasing ϵ_{max} to 0.5. The success of this test with larger ϵ_{max} compared with the above mentioned two tests, where ϵ_{max} was 0.43, revealed that

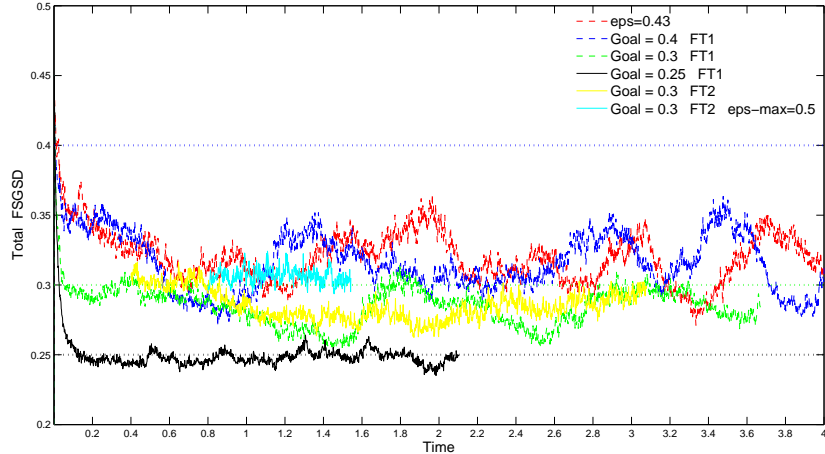


Figure 3.1: Time-history of total fraction SGSD.

the upper bound of the interval for allowable threshold variations was not large enough to increase the SGS dissipation accordingly, which implies that with $\epsilon \in [0.2, 0.43]$ flow was over resolved. Therefore, to achieve a FSGSD greater than the average of FSGSD corresponding to constant-thresholding at a certain $\epsilon_{\text{constant-thresholding}}$, it is required to set the $\epsilon_{\max} > \epsilon_{\text{constant-thresholding}}$. This is further confirmed by considering the case with the goal set to 0.25, which illustrates how precisely the spatially variable thresholding methodology can maintain II at a priori defined level. In addition, when ϵ_{\max} is set up high enough, the SGS dissipation approaches the desired level within few eddy turnover times.

The time history of TAF and τ_ϵ^{-1} are shown in Fig. 3.2. The relaxation time parameter for FT2, τ_ϵ , is approximately one-tenth of the large eddy turnover time, $\tau_{\text{eddy}} = \frac{u'^2}{\langle \varepsilon \rangle} = \frac{\frac{2}{3}K}{2KQ} = \frac{1}{3Q} = \frac{1}{18}$. While the relaxation time parameter for FT1, $C_{f_\epsilon} \text{TAF}^{-1}$, is between one-third and one-fourth of τ_{eddy} . That is, FT2 has as much as 2 to 3 times faster response compared with FT1. This faster time response was able to partially recover the FSGSD. This improvement reveals the importance of very localized and fast mechanisms for the forcing term. The time-averaged term in FT1 destroys the localized Lagrangian nature of the algorithm; however, to smear out the effect of possible very

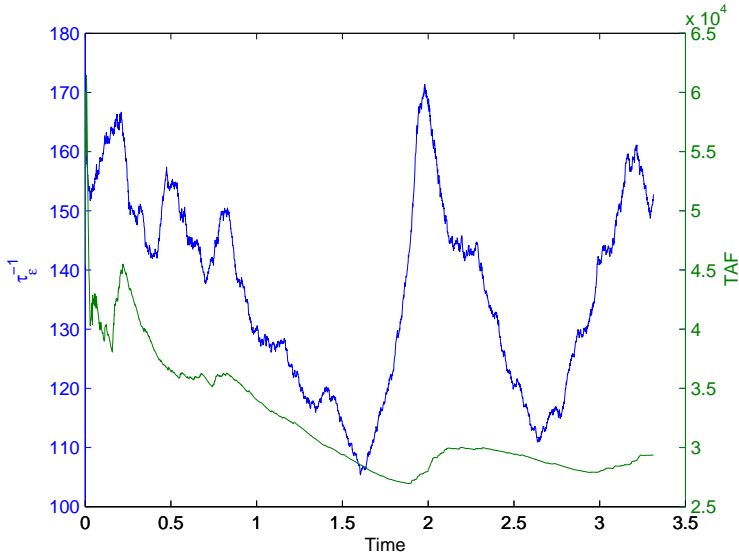


Figure 3.2: Time-history of TAF and τ_ϵ^{-1} .

$$\begin{aligned} \text{Relaxation Time Parameter for FT1 : } C_{f_e} \text{TAF}^{-1} &\approx \frac{1}{3 \text{ or } 4} \tau_{\text{eddy}} \left(\frac{1}{75} \right) \\ \text{Relaxation Time Parameter for FT2 : } \tau_\epsilon &\approx \frac{1}{10} \tau_{\text{eddy}} \left(\frac{1}{170} \right) \end{aligned}$$

localized FSGSD values, it is recommended to have some averaging mechanism. Hence, another approach, which is currently under investigation, is to track the forcing term itself within a Lagrangian frame so that the forcing term inherits the history of the flow evolution.

Analysis of spatially variable thresholding SCALES by means of the localized dynamic kinetic-energy model (LDKM) – in which either Bardina-like or Germano-like approach is exploited for the dynamical evaluation of both turbulent eddy-viscosity and SGS energy dissipation model coefficients – to close the filtered momentum equations is the subject of further investigations.

Time history of number of active wavelets, N_{wlt} , shows that for small goal value of 0.25, number of grid points by average is higher while all the other variable thresholding cases inherit approximately the same average of number of active wavelets compared with the constant-threshold case of $\epsilon = 0.43$, Fig. 3.3.

Compression Ratio, $N_{\text{wlt}}/N_{\text{wlt}_{\text{Max}}}$ – which is the ratio of the active wavelets on the adaptive grid to the total available wavelets on the non-adaptive effective grid at

the highest level of resolution or DNS resolution of 256^3 – illustrated a compression of less than 1% at most of the time for all cases except Goal=0.25, Fig. 3.4. Even for Goal=0.25, the compression is retained at less than 2 %. Considering that the sixth order AWCM code is about 3 to 5 times slower per grid point than pseudo-spectral DNS code [8], even the worst case scenario of compression factor of 2%, represents an acceleration of approximately 16 to 10 times with respect to pseudo-spectral DNS. This clarifies the enormous compression, i.e. number one strength of the wavelets in turbulence.

Total Resolved Dissipation, $\langle \varepsilon_{\text{res}} \rangle$, Fig. 3.5, indicates that not necessarily the smaller goal value for FSGSD results in higher resolved dissipation at all time. This is because of the fact that the continuous coupling between the dissipation and grid-adaptation results in continuous adjustment of resolved dissipation as discussed before by refining or coarsening the grid and as a result at some time/locations it may affect the amplitude of the resolved dissipation differently. Therefore, one can not make such a judgement whether the lower FSGSD goal value means the the higher resolved dissipation throughout the spatial/time space. This argument is valid for the Total SGS Dissipation, $\langle \Pi \rangle$, and Total Resolved+SGS Dissipation, $\langle \varepsilon_{\text{res}} \rangle + \langle \Pi \rangle$, as illustrated in Figures 3.6 and 3.7 respectively.

Taylor Microscale Reynolds Number, $Re_\lambda = \frac{u' \lambda}{\nu}$, where the Taylor length-scale can be evaluated for isotropic turbulence as $\lambda = (\frac{15\nu u'^2}{\langle \varepsilon \rangle})^{1/2}$, is demonstrated in Fig. 3.8 where the time averaged of each case is also shown.

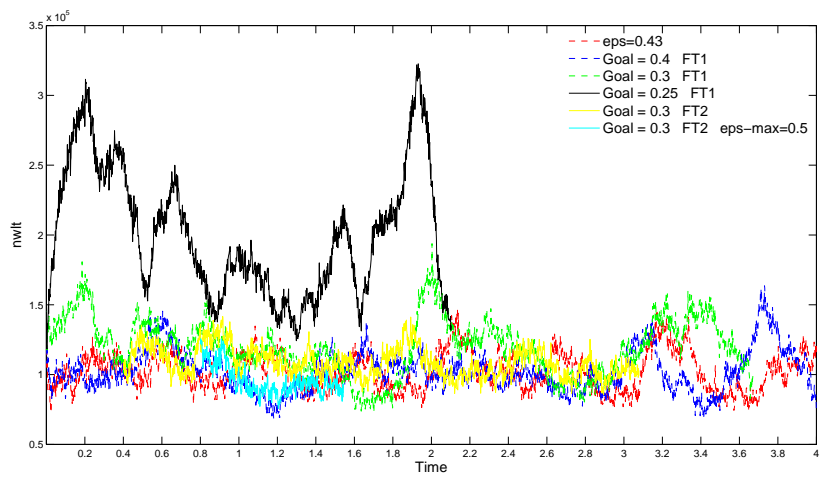


Figure 3.3: Number of Active Wavelets.

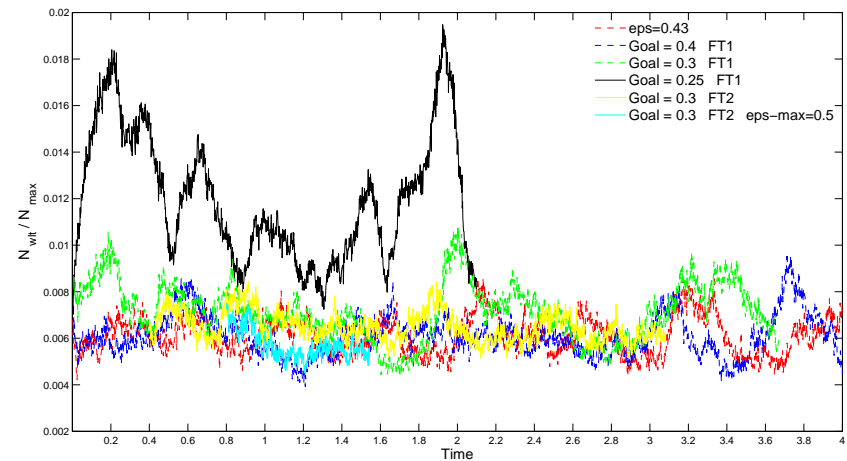
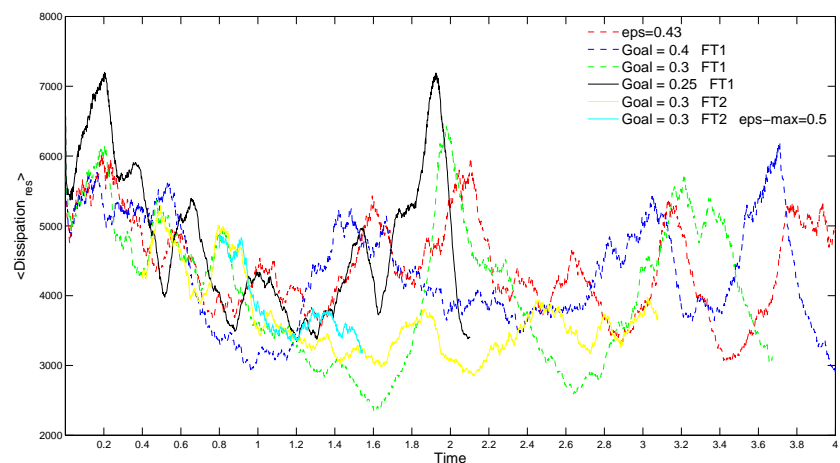
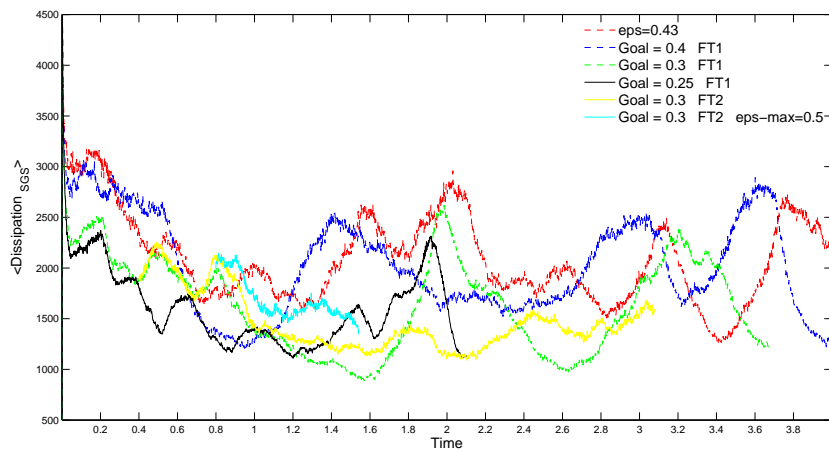
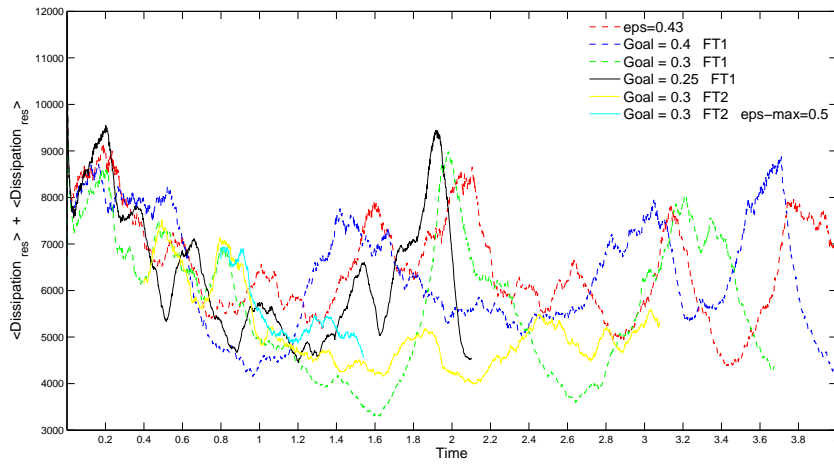
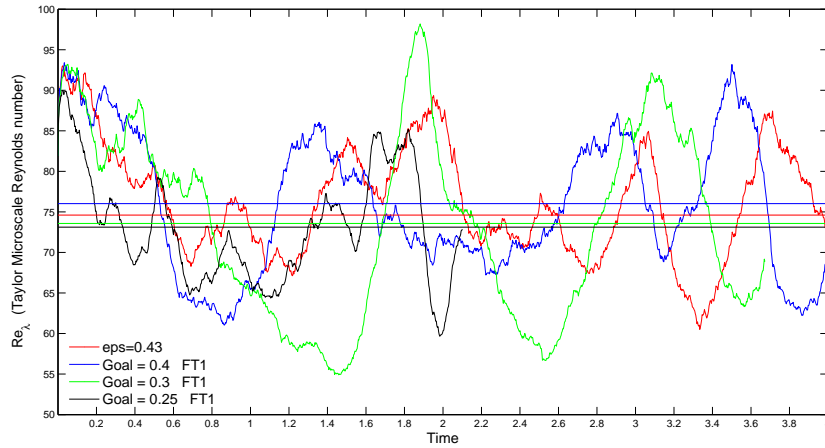


Figure 3.4: Compression Ratio.

Figure 3.5: Total Resolved Dissipation, $\langle \varepsilon_{\text{res}} \rangle$.

Figure 3.6: Total SGS Dissipation, $\langle \Pi \rangle$.Figure 3.7: Total Resolved+SGS Dissipation, $\langle \varepsilon_{\text{res}} \rangle + \langle \Pi \rangle$.Figure 3.8: Taylor Microscale Reynolds Number, Re_λ .

To summarize, variable thresholding is a methodology, which provides two-way feedback between the modeled SGS dissipation and the computational mesh in order to maintain a priori defined level of SGS dissipation, namely a prescribed level of turbulence resolution. The feedback is achieved through spatio-temporal variation of the wavelet threshold that follows the evolution of the resolved/unresolved flow structures. The proposed methodology represents a **fully adaptive wavelet thresholding filter** for turbulent flow simulation, where the thresholding level is determined on the fly by tracking the areas of locally significant SGS dissipation (or any other physical quantity).

This methodology has been also tested for external flow applications where forcing term of “characteristic based tracking of epsilon” is constructed based on the magnitude of vorticity or strain rate. The results for incompressible flow around NACA 0015 airfoil show a very robust and fast methodology for adjusting the thresholding-factor based on dynamically important flow characteristics, for instance, the magnitude of vorticity or strain rate (Figure 3.9).

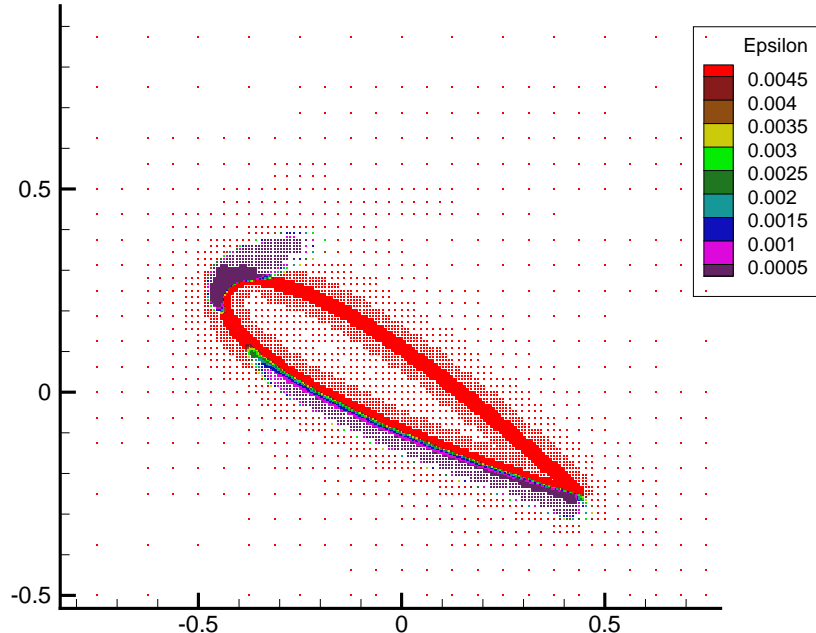


Figure 3.9: Incompressible flow around NACA 0015 at 30° angle-of-attack.

Chapter 4

Perspectives

- **Hybrid Models / Dynamic Load Balancing Implementation / Computational Complexity Study**

The idea of LES and filtering the velocity-field has been a breakthrough in numerical simulation of turbulence yet still have some limitations including large computational cost for high-Reynolds number flows. To overcome the LES shortcomings, there has been a considerable interest in development of hybrid turbulence models. Since they aim at providing better results than RANS without the cost of a complete LES in the entire domain. This is essential for many industrial applications, in particular for high-Reynolds number flows in the presence of walls. The high compression property of the wavelet-based decomposition is a promising feature which can make very large scale hybrid adaptive wavelet-based DNS/LES/URANS of turbulent flows a reality. This work is an attempt develop a framework for very large-scale parallel hybrid adaptive wavelet-based simulation of turbulence. Two major building blocks required for such a framework are 1) hybrid models within the context of adaptive wavelet-based methods by means of the notion of defining the thresholding-factor of the wavelet threshold filter as a field variable (spatial/temporal variable thresholding); and 2) highly-scalable parallel adaptive wavelet-based PDE solver.

In wavelet based methods in general and particularly in SCALES, implementa-

tion of Hybrid DNS/LES/RANS only requires change of wavelet thresholding-factor with no additional efforts for merging two different solvers. Because, within the context of wavelet-based methods, variable fidelity is achieved by changing the thresholding-factor: very small thresholding-factor corresponds to WDNS, moderately small thresholding-factor corresponds to CVS, larger value of thresholding-factor along with solving the SGS models result in SCALES, and much larger value of thresholding-factor for solving Unsteady Reynolds Averaged Navier-Stokes equations lead to WURANS[26] (wavelet-based URANS). Hence, a careful combination of WDNS, CVS, SCALES, and WURANS in a systematic manner can lead to fully adaptive wavelet-based hybrid method.

Transition from WDNS to CVS is very straightforward since it can be controlled only by change of thresholding-factor. Transition from SCALES to CVS can be performed differently. Three main possibilities are: 1) Utilizing SGS model to control SGS dissipation (which has already been discussed) at all time throughout the entire spatial space; 2) instead of solving SGS model, at the CVS level, local kinetic energy of the last band can be monitored; and 3) instead of solving SGS model, at the CVS level, a virtual dissipation – defined analogous to the SGS dissipation – can be monitored. Since most of the dissipation occur at the Kolmogorov scale, dissipation is more smooth and pronounced; however, the kinetic-energy is more noisy at the Kolmogorov scale. This implies that dissipation can be a better measure to identify whether or not we are in the Inertial range, consequently the third (and first) approaches seem to be more practical. On the other hand, the second approach is easier to implement than the third method. Therefore, first approach is the most realistic and easiest technique, in spite of the fact that it requires solving SGS equations at all times everywhere. As a result, transition from SCALES to CVS can also be defined

based on change of thresholding-factor.

The transition from SCALES to WURANS is challenging since it requires switching between SGS models and turbulence models in addition to change of thresholding-factor. Although this can also be handled within one framework using the self-adapting turbulence models[32]. The advantage of these kind of self-adapting models is that they are sufficiently powerful to model the turbulence at any mesh resolution since the classic LES models based on the Smagorinsky approach are limited to meshes that lie in the Inertial range. This is because they all assume that the relevant length scale for the model is the mesh size. In the inertial range this assumption holds, but when the mesh is very coarse – in the energy containing range – or very fine – in the DNS range – this assumption is incorrect[29] and the classic LES approach and its variations like dynamic modeling are fundamentally flawed[32]. Since SCALES is resolving the most energetic structures (either small- or large-scale), in case of using local dynamic energy-based eddy-viscosity models, this problem is in fact less pronounced. Within SCALES framework, due to self-adaptive nature of wavelets, different possibilities can be considered, like a combination of both SGS models and turbulence models with some decaying function of thresholding-factor as a multiplier for turbulence models to mimic their effects while thresholding is decreasing.

Therefore, it is evident that the main requirement for implementation of hybrid wavelet-based models are the capability to dynamically change the thresholding-factor based on instantaneous flow realization. The idea of temporal/spatial varying thresholding has been proposed in the Chapter 2 and its promising initial results are demonstrated within the context of forced homogeneous turbulence in Chapter 3. That is to say, the first aforementioned objective has already

been developed. However, both large-scale simulations and large Reynolds numbers studies require scalable parallel code. Therefore, the main objective at the moment is to develop a parallel variable fidelity adaptive wavelet-based solver with hybrid models for both forced homogeneous turbulence and external flow applications.

The parallel algorithm for the adaptive wavelet collocation method and parallel integrated environment for variable fidelity adaptive multiscale modeling and simulation of turbulence have already been developed in our group. Several partitioning approaches with different user controls are implemented (Figure 4.1). More advanced Zoltan[10, 2, 3, 4, 11, 5] library based partitions provide nearly optimal load balancing. In short, for the geometric simultaneous partitioning all spatial directions of the domain are divided simultaneously. The major deficiency of that approach is poor load balancing for a non-uniform wavelet distribution. For the geometric sequential partitioning, the domain is subdivided by planes normal to the first axis on rounded to the nearest integer $\sqrt[d]{P}$ sub-domains, where d is the problem dimension and P is the total number of processors. The available P processors are distributed among these sub-domain according to the number of active wavelets inside each of the sub-domains. This recursion step is repeated d times to get the final partitioning. It may deliver not quite an optimal load balancing, though it may be more usable for non-uniform wavelet distributions across the domain. For significantly non-uniform wavelet distribution, the domain is partitioned using Zoltan partitioning library by Sandia National Laboratories (Figure 4.1).

Dynamic load balancing is implemented via domain repartitioning during grid adaptation step and reassigning tree data structure nodes to the appropriate processors. User provides an imbalance tolerance vector to trigger the repar-

titioning if necessary. Depending on the imbalance of wavelet distribution a different kind of repartitioning is performed. Highly imbalanced data will be partitioned without considering initial decomposition, moderately imbalanced repartitioned while trying to stay close to the current decomposition, and nearly balanced will be refined by small changes only. Three dimensional example of dynamic load balancing for the 3D simulations of the Convection-Diffusion of rotating ellipsoids is presented in Figure 4.2.

The preliminary studies of the code scalability have been performed for the CVS (thresholding-factor $\epsilon = 0.2$) of linearly forced ($C_f = 6.6$) homogeneous turbulence at $Re_\lambda = 190$ on an adaptive grid corresponds to 1024^3 (at the highest level of resolution) using geometric sequential partitioning (fixed partitioning), Figure 4.3. The scalability studies confirm that parallel code even without dynamic load balancing is scalable with the speedup monotonically increasing with approximately the same slope (nearly linearly scalable up to 128 processors), but saturated at 256 processors. This early saturation is because of huge miss-balance due to the lack of dynamic load balancing.

As mentioned above, the DLB capability via Zoltan library has been implemented as part of this work; although, the implementation has not been flawless and main emphasis at the moment is on debugging the DLB feature of the code since for turbulence applications, drastic relocation of the active wavelets definitely necessitates the need for DLB. The detailed results of the scalability in case of DLB – including speedup based on time-integration, parallel-communication, parallel-migration, and grid-adaptation timers as well as miss-balance data – will be addressed in the final report of this dissertation.

Once the DLB feature be fully functional, the next major objective to meet, is computational complexity studies of the proposed hybrid WDNS/CVS/SCALES/

URANS methodology. It is believed that the current framework will make it possible to perform such studies on very large domain and at large Reynolds numbers, i.e. once the dynamic load balancing for this fully adaptive algorithm implemented completely, with the aim of enormous compression of wavelets (e.g. 99%), the wavelet-based fully adaptive LES and hybrid WDNS/CVS/SCALES/WURANS of turbulence at high Reynolds number will be soon available. This will materialize the very long time dream of a fully adaptive hybrid turbulence simulation using a well established wavelet-based method (SCALES).

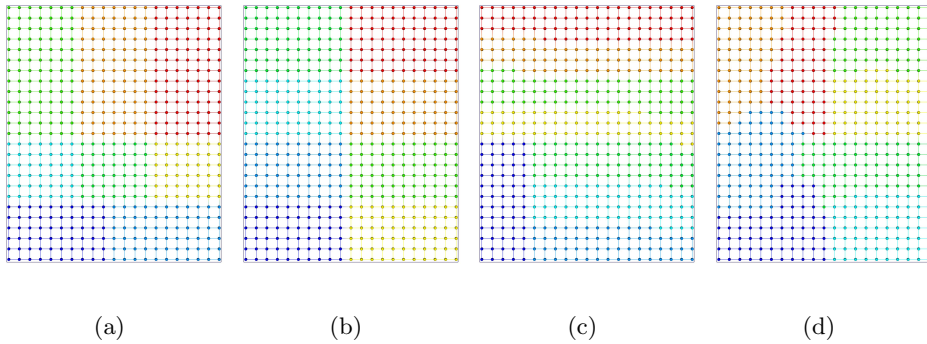


Figure 4.1: Domain partitioning: (a) geometric simultaneous, (b) geometric sequential, (c) Zoltan geometric, (d) Zoltan hypergraph.

- **Solver Improvements**

A basic result of external flow application has shown in Chapter 3. Further progresses in the external flow studies has been captive of some numerical instabilities initiated at the corner points of the domain which are caused by our current matrix-free solver. In an ongoing effort, through implementation of highly-scalable linear solvers of the Trilinos packages [33, 19, 20, 22, 21, 18], it is planned to remove this limitation shortly.

- **Lagrangian Averaged of Forcing**

Another ongoing investigation as discussed in the previous chapter is to track the

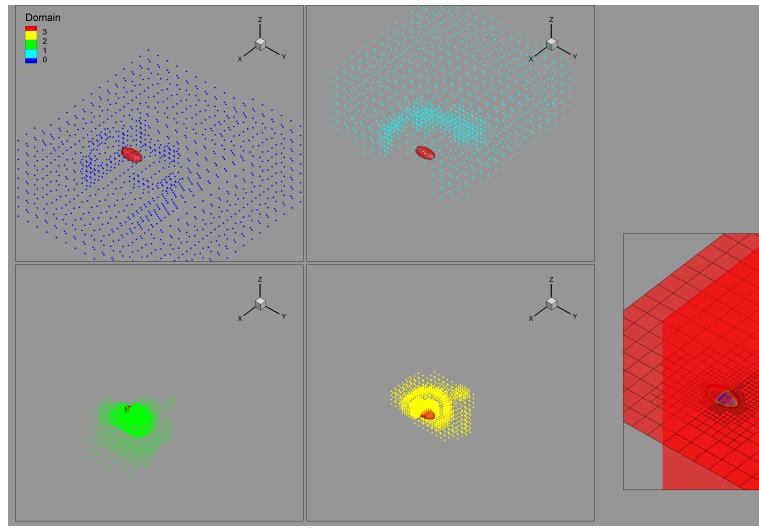


Figure 4.2: Dynamic Load balancing using Zoltan hypergraph domain partitioning for Convection-Diffusion of Rotating Ellipsoids.

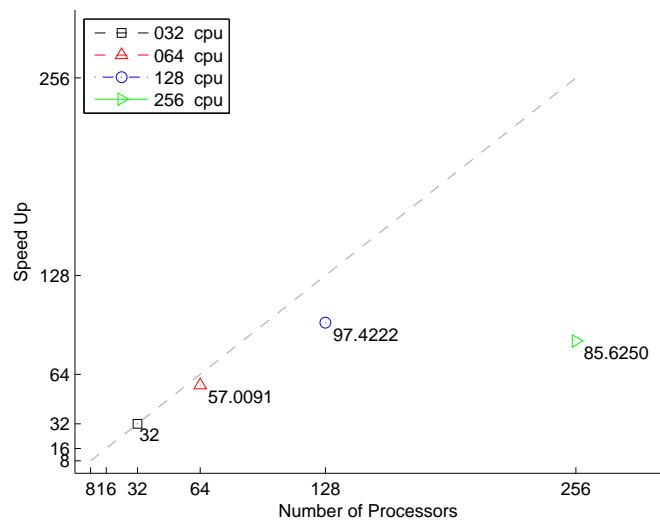


Figure 4.3: Parallel Speedup for CVS $\epsilon = 0.2$ $\nu = 0.015$ $C_f = 6.6$ $Re_\lambda = 190$ 1024^3 using geometric sequential partitioning.

forcing term itself within a Lagrangian frame so that the forcing term inherits the history of the flow evolution, i.e., analogous to the FT2, the forcing is defined based on Lagrangian Averaged of Forcing, \mathcal{I}_F ,

$$\text{forcing}_{\text{term}} = \epsilon^{\text{old}} (\mathbf{x} - \bar{\mathbf{u}}^> \epsilon \Delta t, t) \underbrace{C_{f_\epsilon}}_{400} \frac{1}{\tau_\epsilon} \frac{1}{\mathcal{I}_F} (\Pi - \varepsilon_{\text{res}} \frac{\text{Goal}}{1 - \text{Goal}}), \quad (4.1)$$

where the Lagrangian Averaged of Forcing defined as the statistical average of the forcing, $F(\mathbf{x}(\tau), \tau)$,

$$\mathcal{I}_F(\mathbf{x}, t) = \frac{1}{\tau_\epsilon} \int_{-\infty}^t e^{\frac{\tau-t}{\tau_\epsilon}} F(\mathbf{x}(\tau), \tau) d\tau. \quad (4.2)$$

Similar to the threshold-factor, the Lagrangian representation of $F(\mathbf{x}(\tau), \tau)$, is tracked using the Lagrangian Path-Line Diffusive Averaging approach:

$$\partial_t \mathcal{I}_F + \bar{u}_j^> \epsilon \partial_{x_j} \mathcal{I}_F = -\frac{1}{\tau_\epsilon} (F_{\text{local}} - \mathcal{I}_F) + \nu_{\mathcal{I}_F} \partial_{x_j x_j}^2 \mathcal{I}_F, \quad (4.3)$$

where the local forcing is defined as follows:

$$F_{\text{local}} = \Pi - \varepsilon_{\text{res}} \frac{\text{Goal}}{1 - \text{Goal}}. \quad (4.4)$$

Therefore, the forcing, $F(\mathbf{x}(\tau), \tau)$, also follows the local flow structures as they evolve in space and time.

• Stochastic SGS Models

As discussed in Chapter 1, in the current implementation of the SCALES methodology, only the effect of the “minority deterministic coherent SGS modes” on the “deterministic most energetic coherent structures” are modeled by the “deterministic SGS models”. However, it is of great interest to be able to model the effect of the “majority stochastic incoherent SGS modes” on the “deterministic most energetic coherent structures” as well by means of “stochastic

SGS models". The author feels in infancy stage of understanding the required mathematical background: theoretical/numerical Stochastic Partial Differential Equations (SPDE); however, he hopes he can at least make some preliminary progresses toward understanding the Stochastic SGS models and their implementation within SCALES framework.

- **Uncertainty Quantification Studies**

It is said that among the the future directions of the computational sciences, main concern will be uncertainties issues. Keeping this in mind, another dream is to be able to fine-tune the deterministic SGS models based on the Uncertainty Quantification (UQ) concepts. Hence, it is hoped to be engaged in learning process of the UQ concepts and its possible advantages in instantaneous corrections/adjustments of the SGS models. The UQ based adjustment of the time-relaxation-parameter and forcing-term of the threshold-factor Lagrangian evolution, as well as UQ based adjustment of hybrid model transition algorithm (when/where to switch among WDNS/CSV/SCALES) are also on the wish-list.

Finally, in words of Marcel Lesieur [25],

It might finally happen that this would be only a necessary transition stage toward the definition of new fluid dynamical concepts which would render obsolete and useless the complicated analytical and numerical techniques which helped create them.

Bibliography

- [1] George Papanicolaou from stanford university in an interview with science watch correspondent Gary Taubes.
- [2] Erik Boman, Karen Devine, Lee Ann Fisk, Robert Heaphy, Bruce Hendrickson, Vitus Leung, Courtenay Vaughan, Umit Catalyürek, Doruk Bozdag, and William Mitchell. Zoltan home page. <http://www.cs.sandia.gov/Zoltan>, 1999.
- [3] Erik Boman, Karen Devine, Lee Ann Fisk, Robert Heaphy, Bruce Hendrickson, Courtenay Vaughan, Umit Catalyürek, Doruk Bozdag, William Mitchell, and James Teresco. Zoltan 3.0: Parallel Partitioning, Load-balancing, and Data Management Services; User's Guide. Sandia National Laboratories, Albuquerque, NM, 2007. Tech. Report SAND2007-4748W http://www.cs.sandia.gov/Zoltan/ug_html/ug.html.
- [4] Erik Boman, Karen Devine, Lee Ann Fisk, Robert Heaphy, Bruce Hendrickson, Courtenay Vaughan, Umit Catalyürek, Doruk Bozdag, William Mitchell, and James Teresco. Zoltan 3.0: Parallel Partitioning, Load-balancing, and Data Management Services; Developer's Guide. Sandia National Laboratories, Albuquerque, NM, 2007. Tech. Report SAND2007-4749W, http://www.cs.sandia.gov/Zoltan/dev_html/dev.html.
- [5] U.V. Catalyürek, E.G. Boman, K.D. Devine, D. Bozdag, R.T. Heaphy, and L.A. Riesen. Hypergraph-based dynamic load balancing for adaptive scientific computations. In Proc. of 21st International Parallel and Distributed Processing Symposium (IPDPS'07). IEEE, 2007. Best Algorithms Paper Award.
- [6] Giuliano De Stefano, Daniel E. Goldstein, and Oleg V. Vasilyev. On the role of sub-grid scale coherent modes in large eddy simulation. Journal of Fluid Mechanics, 525:263–274,, 2005.
- [7] Giuliano De Stefano and Oleg V. Vasilyev. A fully adaptive wavelet-based approach to homogeneous turbulence simulation. Physics of Fluids, submitted, 2010.
- [8] Giuliano De Stefano and Oleg V. Vasilyev. Stochastic coherent adaptive large eddy simulation of forced isotropic turbulence. Journal of Fluid Mechanics, 646:453–470, 2010.

- [9] Giuliano De Stefano, Oleg V. Vasilyev, and Daniel E. Goldstein. Localized dynamic kinetic-energy-based models for stochastic coherent adaptive large eddy simulation. *Physics of Fluids*, 20:045102.1–045102.14, 2008.
- [10] Karen Devine, Erik Boman, Robert Heaphy, Bruce Hendrickson, and Courtenay Vaughan. Zoltan data management services for parallel dynamic applications. *Computing in Science and Engineering*, 4(2):90–97, 2002.
- [11] Karen D. Devine, Erik G. Boman, Robert T. Heaphy, Rob H. Bisseling, and Umit V. Catalyurek. Parallel hypergraph partitioning for scientific computing. IEEE, 2006.
- [12] Marie Farge and Gabriel Rabreau. Transformee en ondelettes pour detecter et analyser les structures coherentes dans les ecolements turbulents bidimensionnels. *C. R. Academie des Sciences de Paris, serie II*(307):1479–1486, 1988.
- [13] Marie Farge and Kai Schneider. Coherent vortex simulation (cvs), a semi-deterministic turbulence model using wavelets. *Flow, Turbulence and Combustion*, 6:393–426, 2001.
- [14] Marie Farge, Kai Schneider, and Nicholas K.-R. Kevlahan. Non-gaussianity and coherent vortex simulation for two-dimensional turbulence using an adaptive orthogonal wavelet basis. *Physics of Fluids*, 11(8):2187–2201, 1999.
- [15] S. Ghosal, Thomas S. Lund, Parviz Moin, and K. Akselvoll. A dynamic localization model for large-eddy simulation of turbulent flows. *Journal of Fluid Mechanics*, 286:229255, 1995.
- [16] Daniel E. Goldstein and Oleg V. Vasilyev. Stochastic coherent adaptive large eddy simulation method. *Physics of Fluids*, 16(7):2497–2513, 2004.
- [17] Daniel E. Goldstein, Oleg V. Vasilyev, and Nicholas K.-R. Kevlahan. Cvs and scales simulation of 3d isotropic turbulence. *Journal of Turbulence*, 6(37):1–20, 2005.
- [18] Michael Heroux, Roscoe Bartlett, Vicki Howle, Robert Hoekstra, Jonathan Hu, Tamara Kolda, Richard Lehoucq, Kevin Long, Roger Pawlowski, Eric Phipps, Andrew Salinger, Heidi Thornquist, Ray Tuminaro, James Willenbring, and Alan Williams. An Overview of Trilinos. Technical Report SAND2003-2927, Sandia National Laboratories, 2003.
- [19] Michael A. Heroux, Roscoe A. Bartlett, Vicki E. Howle, Robert J. Hoekstra, Jonathan J. Hu, Tamara G. Kolda, Richard B. Lehoucq, Kevin R. Long, Roger P. Pawlowski, Eric T. Phipps, Andrew G. Salinger, Heidi K. Thornquist, Ray S. Tuminaro, James M. Willenbring, Alan Williams, and Kendall S. Stanley. An overview of the trilinos project. *ACM Trans. Math. Softw.*, 31(3):397–423, 2005.
- [20] Michael A. Heroux and James M. Willenbring. Trilinos Users Guide. Technical Report SAND2003-2952, Sandia National Laboratories, 2003.
- [21] Michael A. Heroux, James M. Willenbring, and Robert Heaphy. Trilinos Developers Guide. Technical Report SAND2003-1898, Sandia National Laboratories, 2003.

- [22] Michael A. Heroux, James M. Willenbring, and Robert Heaphy. Trilinos Developers Guide Part II: ASCI Software Quality Engineering Practices Version 1.0. Technical Report SAND2003-1899, Sandia National Laboratories, 2003.
- [23] Kai Schneider Jochen Frhlich. Numerical simulation of decaying turbulence in an adaptive wavelet basis. *Applied and Computational Harmonic Analysis*, 3:393–397, 1996.
- [24] Jovan Jovanović. *The Statistical Dynamics of Turbulence*.
- [25] Marcel Lesieur. *Turbulence in Fluids*. 4th edition.
- [26] Qianlong Liu and Oleg V. Vasilyev. Hybrid adaptive wavelet collocation-brinkman penalization method for dns and urans simulations of compressible flow around bluff bodies. *AIAA Paper No. 2006-3206*, 2006.
- [27] T.S. Lundgren. Linearly forced isotropic turbulence. *Annual Research Briefs*, pages 461–473, 2003.
- [28] A. Uno T. Ishihara M. Yokokawa, K. Itakura and Y. Kaneda. 16.4-tflops direct numerical simulation of turbulence by a fourier spectral method on the earth simulator. Baltimore MD, 2002.
- [29] Charles Meneveau and Thomas S. Lund. The dynamic smagorinsky model and scale-dependent coefficients in the viscous range of turbulence. *Physics of Fluids*, 9:3932, 1997.
- [30] Charles Meneveau, Thomas S. Lund, and William H. Cabot. A lagrangian dynamic subgrid-scale model of turbulence. *Journal of Fluid Mechanics*, 319:353–385, 1996.
- [31] AliReza Nejadmalayeri, Oleg V. Vasilyev, Alexei Vezolainen, and Giuliano De Stefano. Spatially variable thresholding for stochastic coherent adaptive les. In accepted for Proceedings of Direct and Large-Eddy Simulation Workshop 8. Eindhoven University of Technology, the Netherlands,, 2010.
- [32] J. Blair Perot and Jason Gadebusch. A self-adapting turbulence model for flow simulation at any mesh resolution. *Physics of Fluids*, 19(11):115105.1–115105.11, 2007.
- [33] Marzio Sala, Michael A. Heroux, and David M. Day. Trilinos Tutorial. Technical Report SAND2004-2189, Sandia National Laboratories, 2004.
- [34] Kai Schneider and Oleg V. Vasilyev. Wavelet methods in computational fluid dynamics. *Annual Review of Fluid Mechanics*, 42:473–503, 2010.
- [35] Oleg V. Vasilyev and Christopher Bowman. Second generation wavelet collocation method for the solution of partial differential equations. *Journal of Computational Physics*, 165:660–693, 2000.
- [36] Oleg V. Vasilyev, Giuliano De Stefano, Daniel E. Goldstein, and Nicholas K.-R. Kevlahan. Lagrangian dynamic sgs model for scales of isotropic turbulence. *Journal of Turbulence*, 9(11):1–14, 2008.